Hexavalent Chromium Induces Expression of Mesenchymal and Stem Cell Markers in Renal Epithelial Cells

Wei-Jen Li,[1] Cheng-Lin Yang,[2] Kuan-Chih Chow,[2,3]* and Ting-Wei Kuo[2]

[1]*Department of Health Beauty, School of Medical and Health Sciences, Fooyin University, Kaohsiung, Taiwan*
[2]*Graduate Institute of Biomedical Sciences, National Chung Hsing University, Taichung, Taiwan*
[3]*Agricultural Biotechnology Center, National Chung Hsing University, Taichung, Taiwan*

Cr(VI) causes severe kidney damage. The patient's renal function could gradually recover by spontaneous kidney regeneration. The molecular effect of Cr(VI) on recovery of kidney cells, however, has not been clearly elucidated. Here we show that Cr(VI) induces expression of mesenchymal and stem cell markers, cell markers, such as paxillin, vimentin, α-SMA, nanog, and CD133 of HK-2 cells. Moreover, Cr(VI) activates epithelial-to-mesenchymal transition (EMT). By revealing that levels of dihydrodiol dehydrogenase were promptly reduced following Cr(VI) challenge, our data suggested that DDH could be involved in a Cr(VI)-related oxidation to generate massive reactive oxygen species and H_2O_2, and to create intracellular hypoxia, which then increased levels of SUMO-1 activating enzyme subunit 2, and sumoylation of eukaryotic elongation factor-2, to mediate the subsequent molecular and cellular responses, e.g., expression of mesenchymal and stem cell markers. Pretreatment with vitamin C reduced Cr(VI)-related cellular effects. However, no evident effect was observed when vitamin C was added following Cr(VI) challenge.

Key words: Cr(VI); DDH; paxillin; vimentin; connexin-43; nanog; CD133; EMT

INTRODUCTION

Hexavalent chromium [Cr(VI)] is a chemical compound that is frequently used in industries manufacturing stainless steel, textile dyes, housing wood products, and paints, as well as in water cooling system of power plants, for anti-corrosion coatings and material preservation purposes (www.osha.gov/SLTC/hexavalent chromium). However, besides inducing cell damages to the skin, intestines, stomach, and kidney, Cr(VI) could also increase carcinogenic risk of the lung, bowels, and kidney (en.wikipedia.org/wiki/Hexavalent chromium). Historically, prevention of inhaling chromium fumes had markedly decreased Cr(VI)-related lung cancer in industrial workers (monographs.iarc.fr/ENG/Monographs/vol100C/mono100C-9.pdf). An elegant study, nonetheless, demonstrated that urinary chromium levels of Finnish welding workers were elevated and exceeded the governmental recommended concentration, in particular the smokers, implicating that chromium particulates deposited in lungs could be absorbed into the circulation and carried to the kidney [1]. Interestingly, in the USA, the area that had notorious industrial pollutions also had the highest occurrence rate of end-stage renal disease [2]. A recent epidemiological study of Oinofita, Greece, where the drinking water was heavily contaminated with Cr(VI), further showed that the prevalence of the primary liver, testicular, kidney, and lung cancer-related deaths was significantly higher than the other areas, clearly supporting the facts that in addition to vaporized solid chromium particles, soluble Cr(VI) could induce carcinogenesis as well [3].

As noted in a well-documented review, after a transient exposure to massive Cr(VI), the first symptom of acute kidney damage was a marked decrease of urine flow rate (the oligouric phase, urine output

Abbreviations: ATAD3A, ATPase family, AAA domain containing 3A; AMPK, AMP-activated protein kinase; AO, acridine orange; α-SMA, alpha smooth muscle actin; CI_{50}, half maximal inhibitory concentration; Cr(III), trivalent chromium; Cr(VI), hexavalent chromium; CX-43, connexin-43; DDH, dihydrodiol dehydrogenase; DRP1, dynamin-related protein 1; eEF-2, eukaryotic elongation factor-2; EMT, epithelial-to-mesenchymal transition; HGF, hepatocyte growth factor; HIF-1α, hypoxia-inducible factor 1 alpha; KTE, kidney tubular epithelial; Mfn-2, mitofusin-2; MSC, mesenchymal and stem cell; ROR, reductive/oxidative reactions; ROS, reactive oxygen species; SAE2, SUMO-1 activating enzyme subunit 2; TrxR, thioredoxin reductases.

Conflicts of interest: The authors indicate no potential conflicts of interest.

W.J.L., experiment manipulations, data analysis, and manuscript preparation; C.L.Y., experiment manipulations and data analysis; C.L.Y. and T.W.K., RT-PCR, ELISA and raise of monoclonal antibodies; K.C.C. perception of the idea, experimental design, guidance, manuscript preparation, and writing.

Grant sponsor: National Science Council; Grant number: NSC 102-2320-B-005-006; Grant sponsor: Comprehensive Academic Promotion Projects; Grant number: NCHU 1025025

*Correspondence to: Graduate Institute of Biomedical Sciences, National Chung Hsing University, Taichung 40227, Taiwan.

Received 29 July 2014; Revised 11 November 2014; Accepted 26 November 2014

DOI 10.1002/mc.22268

Published online 24 January 2015 in Wiley Online Library (wileyonlinelibrary.com).

<200 mL/day in adults), and followed by a polyuric phase (urine output >3 L/day) [4]. These clinical signs unmistakably suggested that Cr(VI) could cause severe damage to both nephrons and renal tubules. If patients survived the acute Cr(VI) cytotoxicity, their renal function could gradually recover by spontaneous nephral and tubular regeneration as well as differentiation [5]. Although two types of renal progenitor cells had been identified responsible for the respective nephral and tubular repair [6], the in vitro effect of Cr(VI) on these cells, in particular, the kidney tubular epithelial (KTE) cells, has not been reported.

In this study, we found that Cr(VI) not only introduced cytotoxicity to, but also induced morphological changes of the immortalized kidney tubular epithelial cells, HK-2, showing features of epithelial-to-mesenchymal transition (EMT). We therefore examined expressions of mesenchymal cell markers, such as vimentin, paxillin, and α-smooth muscle actin (α-SMA) [7–9], as well as those of stem cell markers, nanog [10], and CD133 [11], in HK-2 cells. The effect of Cr(VI) on cell growth and EMT was characterized in vitro.

MATERIALS AND METHODS

Materials

Hexavalent Chromium (potassium dichromate solution) and antibodies to β-actin were purchased from Sigma–Aldrich® (Basel, Switzerland). Antibodies to nanog, Poly (ADP-ribose) polymerase (PARP), and vimentin were acquired from Cell Signaling Technology, Inc. (Danvers, MA). Antibodies to *alpha smooth muscle actin* (α-SMA) and paxillin were obtained from Thermo Fisher Scientific, Inc. (Waltham, MA). Antibodies to CD-133, Src, and connexin-43 (CX-43) were respectively bought from Biorbyt (Cambridge, Cambridgeshire, UK), Calbiochem-Merck Biosciences, Merck Millipore (Taipei, Taiwan), or Santa Cruz Biotechnology, Inc. (Dallas, TX). Monoclonal antibodies to AIF, ATAD3A, DDH, DRP1, eEF2 [12–16], Mfn-2, and SAE2 (Supporting information Figure S1) were home-raised against the respective recombinant protein. The monoclonal antibodies were characterized by immunoblotting, which recognized the proteins with particular molecular weight in a gel electrophoresis of the A549 cell lysates. Proteins isolated by immunoprecipitation were further analyzed by MALDI-TOF, and the identity of the protein was determined by peptide mass fingerprint-matching to the specific protein sequence in the database of GenBank (www.ncbi.nlm.nih.gov/genbank) and UniProtKB/Swiss-Prot (www.ebi.ac.uk/swissprot/).

Cell Culture

HK-2 cells (ATCC#: CRL-2190) were used for the in vitro effect evaluation of Cr(VI). HK-2 is a human papilloma virus E6/E7-immortalized human kidney cell line derived from proximal tubules. Two lung adenocarcinoma (LADC) cell lines (H838 and A549) [17], which expressed high levels of DDH, were also used in the study. Cells were maintained at 37°C as a monolayer in DMEM/F12 or RPMI-1640 for LADC cells supplemented with 10% fetal calf serum, 100 IU/mL of penicillin, and 100 μg/mL of streptomycin in a humidified 5% CO_2 incubator.

Immunoblotting Analysis

Immunoblotting was performed following the previously described methods [18,19]. Briefly, total cell lysate was prepared by resuspending 5×10^7 cells in 100 μL phosphate-buffered saline, and then mixing with equal volume of 2 × NP-40 lysis buffer [40 mM Tris-HCl, pH 7.6, 2 mM EDTA, 300 mM NaCl, 2 mM phenylmethylsulfonylfluoride (PMSF2%), and NP-40]. Proper amount of loading buffer (50 mM Tris, pH 6.8, 150 mM NaCl, 1 mM PMSF, 1 mM disodium EDTA, 10% glycerol, 5% β-mercaptoethanol, 0.01% bromophenol blue, and 1% SDS) was added to the cell lysate prior to the electrophoresis, which was carried out in a 10% polyacrylamide gel with 4.5% stacking. Following electrophoresis, proteins on the gel were transferred to a nitrocellulose membrane. The membrane was probed with specific antibodies. The signal was amplified by biotin-labeled goat anti-mouse IgG, and peroxidase-conjugated streptavidin. The protein was visualized by exposing the membrane to an X-Omat film (Eastman Kodak, Rochester, NY) with enhanced chemiluminescent reagent (NEN, Boston, MA). Antibodies for β-actin were obtained from Chemicon International (Temecula, CA). The digital images on X-Omat film were processed using Adobe Photoshop 7.0 (http://www.adobe.com/). Intensity of each immunoblotting band was analyzed and quantified using the image-J software (NIH, Bethesda, MD). The blots were stripped using Restore Western Blot Stripping Buffer (Thermo Fisher Scientific, Inc., Rockford, IL) before incubation with other antibodies.

Cr(VI)-Sensitivity Assay

Cr(VI)-sensitivity was measured by a WST-1 assay [20]. Cells were seeded at 100, 1,000, and 5,000 cells/96-well plate 18 h prior to Cr(VI) challenge. Cells were continuously incubated with various concentrations (ranging from 0.1 to 10 μM) of hexavalent chromium. The negative control cells were treated with the phosphate-buffered saline, a solvent for the Cr(VI). Total survival of the cells was determined 72 h following Cr(VI) challenge, and percent survival was estimated by dividing optical absorbance resulted from each test group with that of the control group. Each experiment was done in triplicates, and the optical absorbance was measured by a change of colorless WST-1 to bright yellow color of oxidized WST-1 (BioVision, Mountain View, CA). Oxidation of WST-1 was catalyzed by mitochondrial dehydrogenase [18,19]. The line graph drawing of

cytotoxicity was performed using GraphPad Prism6 statistics software (San Diego, CA).

For determining the effect of Cr(VI) on inducing autophagy, the HK-2 cells were exposed to a serial dilution of potassium dichromate (ranging from 0.25 to 10 μM) for 1–72 h. Culture medium was removed, and the cells were rinsed once with phosphate buffered saline (PBS) before addition of acridine orange (AO) solution to 20 mg/mL PBS. The reaction was carried out at room temperature for 15 min. The AO solution was removed and the cells were rinsed once with PBS before observing under a fluorescence microscope [21].

Immunofluorescence Microscopy

Method for immunofluorescence microscopy had been previously described [12,13]. Concisely, the HK-2 cells, which were grown on aminopropylsilane-coated slides, were fixed with 4% paraformaldehyde at room temperature for 15 min and permeabilized with 0.1% Triton X-100 prior to staining with antibodies to vimentin, a-SMA, paxillin, DRP-1, apoptosis-inducing factor (AIF), or CX-43. After washing off the primary antibodies, the slide was incubated with fluorescein- or Alexa 488-conjugated secondary antibodies (Invitrogen™, Life Technologies, Grand Island, NY). Nuclei of the cells were stained with 4′, 6-diamidino-2-phenylindole (DAPI) and the slides were examined under a fluorescence microscope (Olympus BX51, Tokyo, Japan). Fluorescence was activated using X-Cite® 120 Fluorescence Microscope Illumination System (EXFO, Quebec, Canada).

RNA Extraction and Reverse Transcription Polymerase Chain Reaction (RT-PCR)

Total RNA was extracted from the cultured cells by using an SNAP RNA column (Invitrogen, San Diego, CA). After measuring RNA yield, cDNA was synthesized by AMV reverse transcriptase using oligo random primers. An aliquot of cDNA was then subjected to 35 cycles of PCR. The reaction mixture contained 50 mM Tris (pH 7.2), 1.5 mM $MgCl_2$, 2 μM dNTP, 0.25 μM of 5′ and 3′ primers, respectively, 0.5 U of Taq DNA polymerase (Protech Technology, Taipei, Taiwan), and 2 μL of cDNA (1 μg). PCR was carried out according to the standard procedures: denaturing at 94°C for 30 s, hybridizing at 55°C for 45 s, and elongating at 72°C for 2 min. The amplified PCR products were analyzed in 1% agarose gel and visualized by ethidium bromide staining.

RESULTS

Cr(VI) Suppresses Cell Growth and Induces Morphological Changes of Renal Epithelial HK-2 cells

Addition of Cr(VI) showed cytosuppresive effect in a dose-dependent manner on HK-2 cells, and the half maximal inhibitory concentration (C_{I50}) was estimated to be 1.21 μM (Figure 1A). Cr(VI) induced cell death, as shown by the appearance of cleaved PARP in the Western blot (Figure 1B). Cr(VI) also activated autophagy as demonstrated by the appearance of crimson intracytoplasmic AO-positive vesicles (Figure 1C) in HK-2 cells. However, some cells did not contain AO-positive vesicles. In contrast, the AO-negative cells became elongated, scattered, and crescent shape, resembling the morphology of mesenchymal cells (Figure 1D) [22], and suggesting that Cr(VI) might activate epithelial-to-mesenchymal transition (EMT) of HK-2 cells.

Cr(VI) Increases Expression of Mesenchymal and Stem Cell Markers as Detected by Immunoblotting and Immunofluorescence Microscopy

Interestingly, addition of Cr(VI) dose-dependently increased expression of paxillin, vimentin, and α-SMA (Figure 2A), the essential markers of mesenchymal cells [7–9]. Expression of c-Src, a proto-oncogenic tyrosine-protein kinase, and an intermediate of membrane receptor tyrosine kinase, was also increased. Expression of connexin-43 (CX-43), a structure protein of gap junction which frequently served as a typical non-stem cell surface marker for mature human epithelial cells [23], however, was reduced. The results were confirmed by immunofluorescence microscopy, showing that Cr(VI) enabled HK-2 cells to transform from epithelial to mesenchymal phenotype (Figure 2B).

Previous study revealed that following acute Cr-(VI) cytotoxic damages, patient's renal function could be gradually repaired by spontaneous tubular recovery [4]. Angelotti et al. showed that renal progenitor cells could be accountable for tubular regeneration [6]. It is therefore worth noting that Cr(VI) increased expression of stem cell markers, such as nanog (Figure 2C) and CD133 (Figure 2D) [11], in HK-2 cells.

Cr(VI) Reduces Expression of Dihydrodiol Dehydrogenase (DDH) and Mitofusin-2 (Mfn-2) to Increase Mitochondrial Fragmentation

Although Cr(VI) has chemically higher electric potential, the compulsory reduction of Cr(VI) to Cr(III) involves co-factors as well as effectors on mitochondrial and intracellular membranes [24]. Besides the formation of carcinogenic Cr(III)-DNA adducts, massive reduction of Cr(VI) would obligatorily couple with extensive oxidation of intracellular substrates, which could in turn generate a substantial reactive oxygen species (ROS) and produce oxidative stress in cells [25]. Although Cr(VI) did not evidently affect expression of ATPase family AAA domain-containing 3A (ATAD3A), an essential enzyme for intracellular vesicle transport, Cr(VI) markedly reduced expression of Mfn-2 and DDH (Figure 3A), but increased protein levels of DRP1, suggesting that Cr(VI) might induce abrupt depletion of intracellular oxygen to increase AMP-activated protein kinase (AMPK) activity, which were then responsible for the phosphorylation and nuclear accumulation of

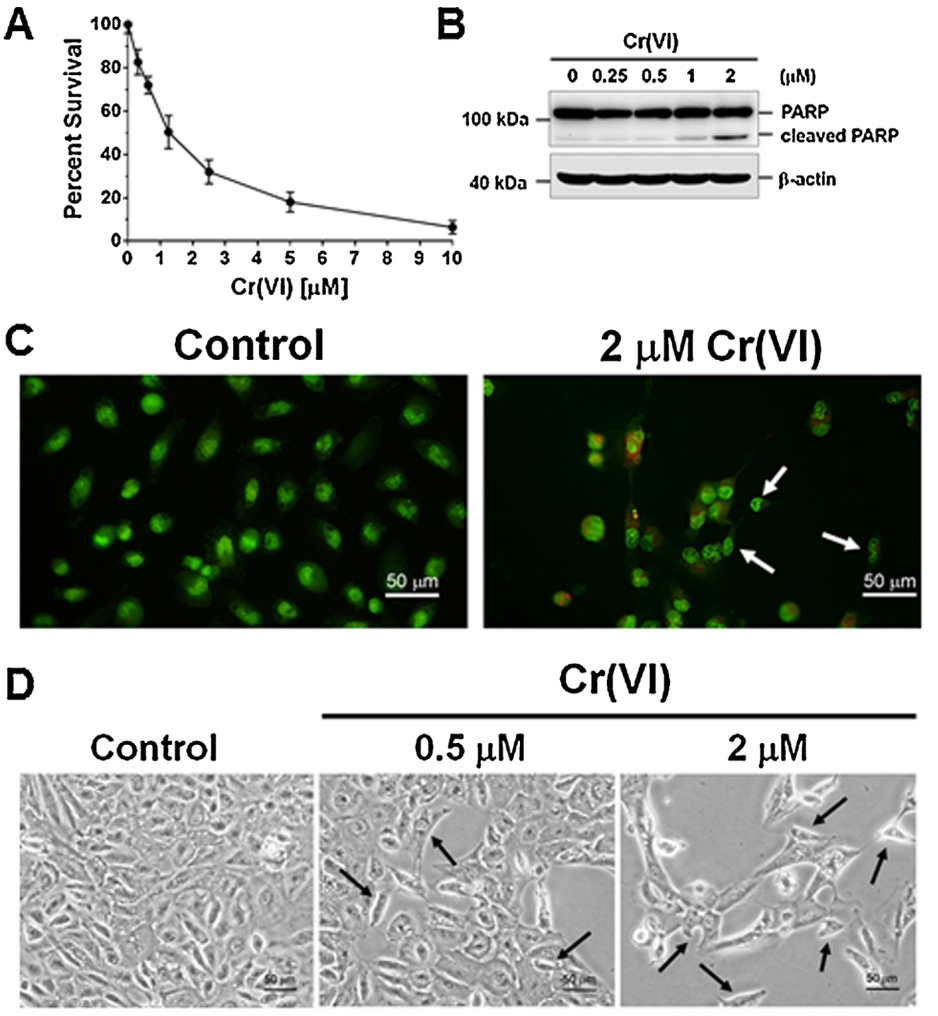

Figure 1. Cr(VI) suppressed cell growth and induced epithelial-to-mesenchymal changes of renal epithelial HK-2 cells. (A) Treatment of HK-2 cells with Cr(VI) suppressed cell growth in a dose-dependent manner. The half maximal inhibitory concentration (C_{I50}) was estimated to be around 1.21 μM. (B) Appearance of the cleaved PARP in a Western blot indicated that Cr(VI) induced cell death. (C) Cr(VI) activated autophagy, as determined by an acridine orange (AO) test. Appearance of the crimson colored intracytoplasmic vesicles indicated that the ingested AO dye was acidified in HK-2 cells. However, some cells did not contain the bright red colored vesicles (white arrows). (D) Morphology of the AO-negative cells was elongated, scattered, and crescent shape (dark arrows), resembling that of mesenchymal cells [22], and implicating that Cr(VI) could activate epithelial-to-mesenchymal transition of HK-2 cells.

DRP1 [15]. As anticipated, Cr(VI) increased nuclear levels of DRP1 (Figure 3B). As silencing of Mfn-2 expression increased mitochondrial fragmentation (Figure 3C), so did Cr(VI) treatment (Figure 3D). Furthermore, subsequent to mitochondrial fragmentation, Cr(VI) also induced nuclear translocation of apoptosis-inducing factor (AIF), a sign of mitochondrial depolarization and apoptosis (Figure 3E).

Cr(VI) Increases Expression of SUMO-1 Activating Enzyme Subunit 2 (SAE2), Eukaryotic Elongation Factor-2 (eEF-2), c-Met and Human Epidermal Growth Factor Receptor-2 (HER-2)

As noted above, addition of Cr(VI) dose-dependently increased expression of several essential markers of mesenchymal and stem cells. By immunoblotting analysis, we found that Cr(VI) also increased expression of eEF2, a vital protein factor that catalyzed translocation of peptidyl-tRNA on ribosome during elongation phase of translation [26], SAE2, c-Met (also named as hepatocyte growth factor receptor, HGFR) and HER-2 in a dose-dependent fashion (Figure 4A). Our prior results showed that eEF2 was frequently sumoylated [16], and the present study revealed that SAE2 and eEF2 were concomitantly up-regulated, indicating that expression of the two proteins could be tied together to increase the sumoylation efficacy, the eEF2 stability, and the synthesis of oxidative stress-associated proteins. Moreover, addition of H_2O_2 increased protein concentrations of SAE2, but reduced

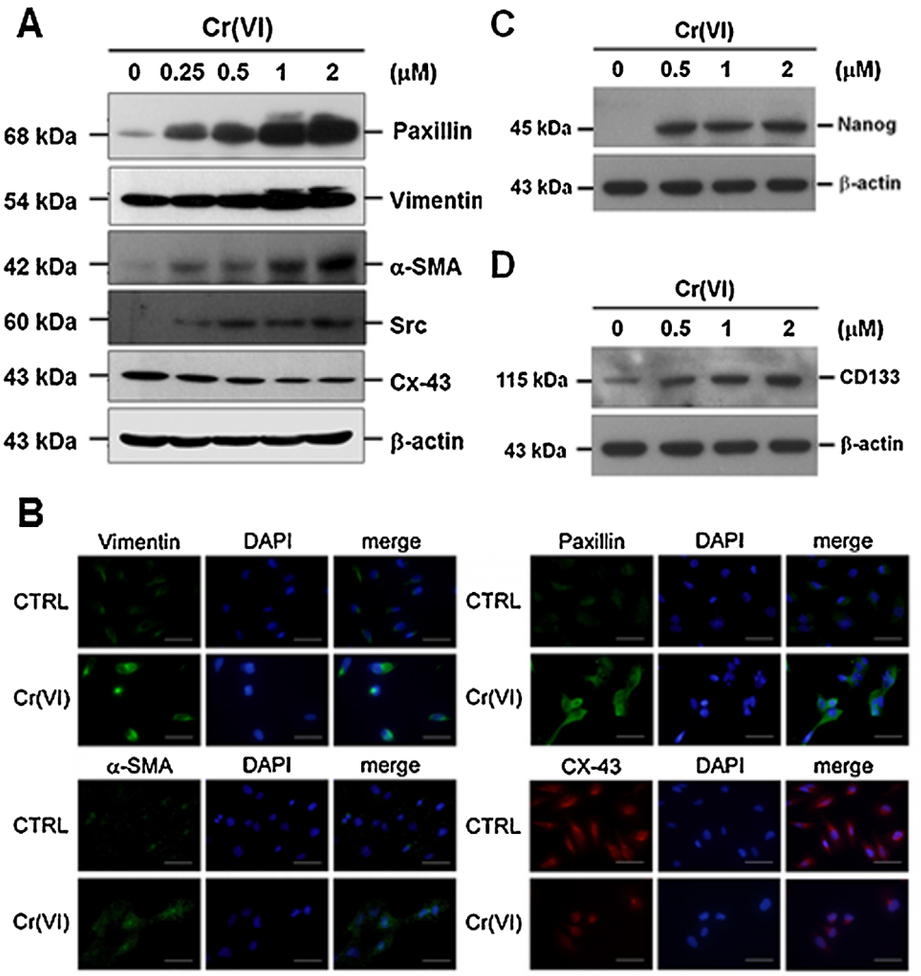

Figure 2. Cr(VI) induced expression of mesenchymal and stem cell markers in HK-2 Cells, as determined by immunoblotting analysis and immunofluorescence microscopy. (A) Cr(VI) dose-dependently increased expression of the essential mesenchymal cell markers, such as paxillin, vimentin, and α-SMA, as well as the proto-oncogenic Src. On the contrary, expression of the mature epithelial cell surface marker, connexin-43 (Cx-43),was reduced. (B) The immunoblotting results were confirmed by images of immunofluorescence microscopy, showing that fluorescent signals of paxillin, vimentin, and α-SMA increased, and those of Cx-43 reduced, suggesting that Cr(VI) could convert HK-2 cells from epithelial to mesenchymal phenotype. (C) Cr(VI) increased expression of stem cell transcription marker, nanog, at low dose. (D) Cr(VI) dose-dependently increased expression of stem cell surface marker, CD133, in HK-2 cells.

those of DDH (Figure 4B), implying that excessive ROS and oxidation level could affect expression of these two enzymes, and substantiating our theory that massive Cr(VI) reduction was accompanied with substantial oxidation, which thereafter generated ROS and caused local hypoxia. Red vesicles (indicating acidified AO) were detected within 1 h following addition of Cr(VI), suggesting that ROS generation and autophagic marker acidification took place very fast inside the cells (Figure 4C). Interestingly, the effect of Cr(VI) on increasing protein levels of paxillin, SAE2, and eEF2 also occurred within 6 h after addition of heavy metal solution, and such effect was augmented 4–10 folds, 48 h post-Cr(VI) challenge (Figure 4D). Knockdown of DDH, however, reduced Cr(VI)-induced expression of mesenchymal and stem cell (MSC) markers (Figure 4E).

To further determine the effect of Cr(VI) on ROS generation and its relationship to MSC marker expression, we found that pretreatment with 100 μM vitamin C (Vit C) decreased Cr(VI)-induced expression of MSC markers (Figure 4F). Addition of vitamin C following Cr(VI) challenge, nonetheless, did not inhibit Cr(VI)-mediated increase of MSC markers expression.

DISCUSSION

Our results show that hexavalent chromium [Cr(VI)] is highly toxic and mediates apoptosis as well as

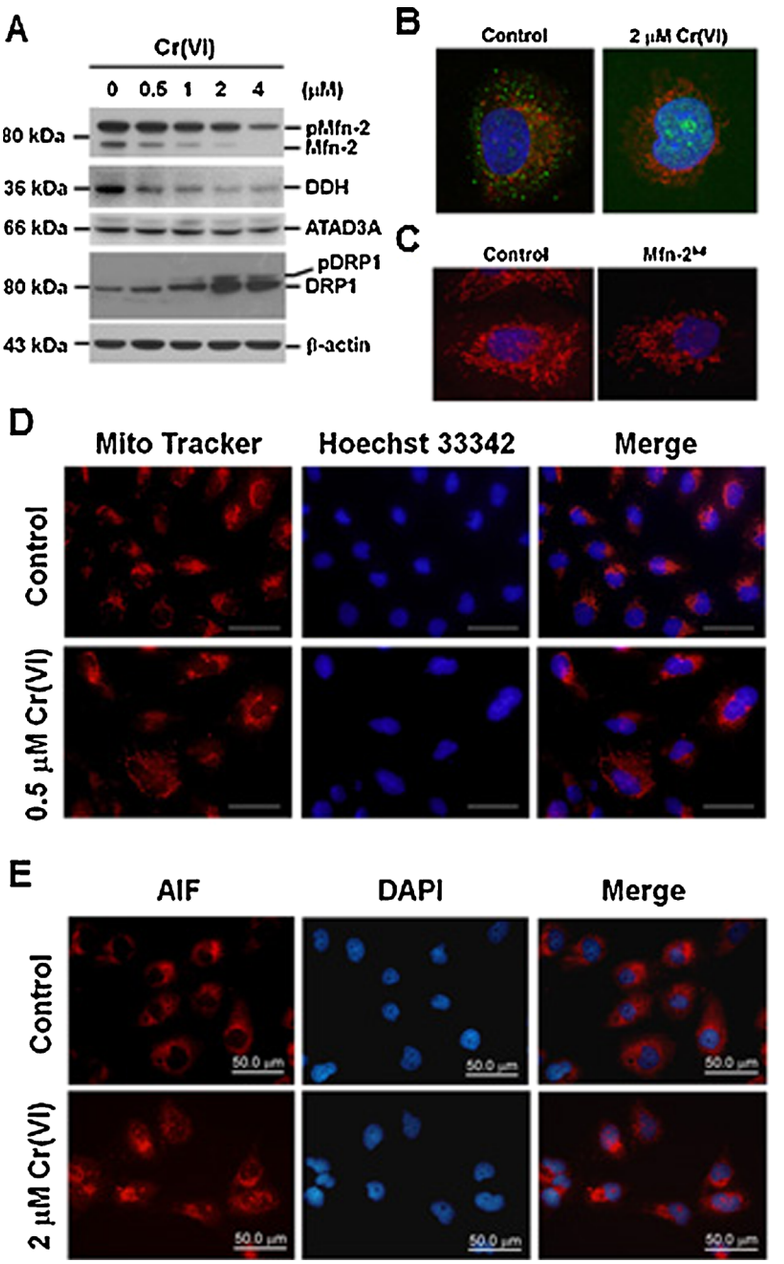

Figure 3. Cr(VI) inhibits expression of mitofusin-2 and dihydrodiol dehydrogenase, as well as induces mitochondrial fragmentation and nuclear translocation of apoptosis-inducing factor. (A) Cr(VI) treatment markedly reduced expression of mitofusin-2 (Mfn-2) and dihydrodiol dehydrogenase (DDH), but increased protein levels of dynamin-related protein 1 (DRP1), suggesting that Cr(VI) could induce rapid intracellular oxygen depletion, and increase AMPK activity to phosphorylate DRP1, which then facilitated nuclear accumulation of DRP1. Cr(VI) challenge, however, did not affect expression of ATPase family AAA domain-containing 3A (ATAD3A), an essential enzyme for intracellular material transport. (B) As anticipated, Cr(VI) increased nuclear levels of DRP1, in particular in regions of nucleoli. (C) As an experimental control, silencing of Mfn-2 expression increased mitochondrial fragmentation. (D) Cr(VI) treatment elevated the frequency of mitochondrial fragmentation in HK-2 cells. (E) As expected, Cr(VI) induced nuclear translocation of apoptosis-inducing factor (AIF), indicating that in addition to mitochondrial fragmentation, Cr(VI) also mediated mitochondrial depolarization and caspase-independent apoptosis.

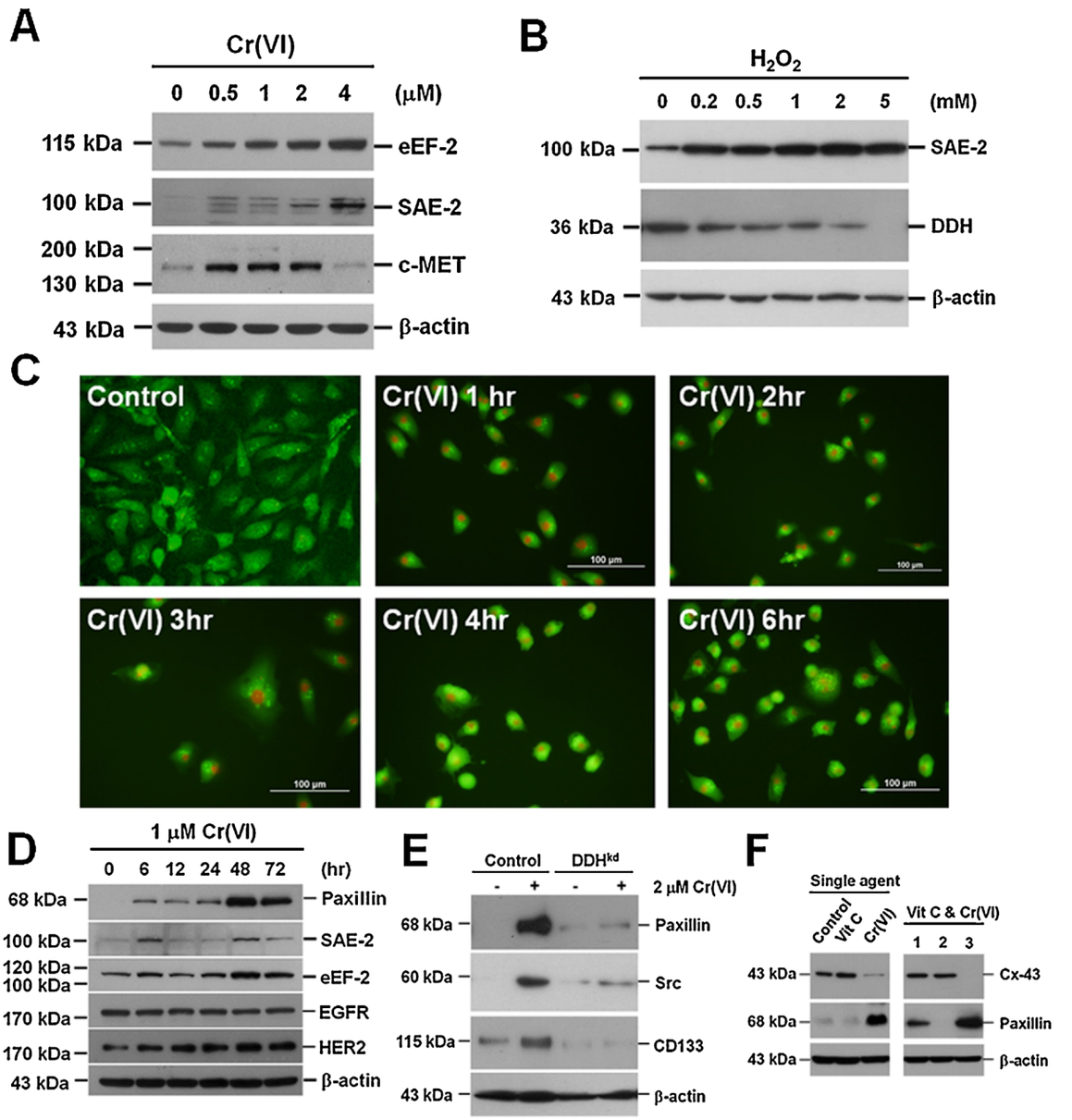

Figure 4. Besides mesenchymal and stem cell markers, Cr(VI) increases expression of SUMO-1 activating enzyme subunit 2, eukaryotic elongation factor-2, and c-Met. (A) As shown above, Cr(VI) increased expression of essential mesenchymal cell and stem cell markers. At the same time, addition of Cr(VI) increased expression of SUMO-1 activating enzyme subunit 2 (SAE2), eukaryotic elongation factor 2 (eEF2), and c-Met (also named as hepatocyte growth factor receptor, HGFR). At 4 μM of Cr(VI), c-Met expression, however, reduced significantly. (B) H_2O_2 dose-dependently increased levels of SAE2. However, exogenously added H_2O_2 reduced DDH levels, supporting our hypothesis that massive Cr(VI) reduction was accompanied by substantial oxidation, which subsequently generated ROS and caused hypoxia. Excessive ROS could oxidize the DDH and accelerate DDH degradation. (C) One hour after addition of Cr(VI), the protonated acridine orange (appeared as red vesicles) was detected, suggesting that generation of ROS and acidification of autophagic marker occurred rapidly inside cells, and the effect persisted. (D) Protein levels of paxillin, SAE2, eEF2, and HER-2 increased within 6 h following Cr(VI) treatment. This effect was augmented 4–10 folds, 48 h post-Cr(VI) challenge. Cr(VI), however, did not evidently influence the expression of epidermal growth factor receptor (EGFR). (E) Silencing of DDH expression inhibited expression of mesenchymal and stem cell (MTC) markers. (F) Addition of 100 μM vitamin C (Vit C) alone did not markedly affect expression of MTC markers (lanes 1 and 2, left panel), though Cr(VI) increased expression of paxillin, but reduced that of Cx-43 (lane 3, left panel). Compared to the control (lane 1, right panel), pre-treatment with 100 μM Vit C for 2 h did not affect Cr(VI)-related decrease of Cx-43 expression, but significantly inhibited Cr(VI)-induced expression of paxillin (lane 2, right panel). Pre-treatment with 2 μM Cr(VI) for 6 h, however, evidently counteracted the inhibitory effect of Vit C on Cr(VI)-induced expression of paxillin (lane 3, right panel).

autophagy in kidney tubular epithelial cells. In vitro, if the cells survived the impact of heavy metal toxicity, Cr(VI), in contrast, could induce expression of MSC markers in addition to the epithelial-to-mesenchymal transition of HK-2 cells.

An elegant study by Myers et al. found that thioredoxin reductases (TrxR) were sensitive to Cr-(VI), suggesting that Cr(VI) could mediate cysteine oxidation in active-site of TrxR and evoke a cascade of reductive/oxidative reaction (ROR) during reduction to Cr(III) [27]. By using fluorescent markers to measure intracellular concentration of $O_2^{-\cdot}$ and H_2O_2, reactive oxygen species (ROS) were mostly detected in perinuclear and juxtanuclear membrane structures [28,29], indicating that Cr(VI)-associated ROR could be occurring in the endoplasmic reticulum (ER) and Golgi apparatus [30,31]. Membrane structures containing oxidized fluorescent markers expanded when cells were treated with superoxide dismutase (SOD). On the contrary, salvage with catalase reduced signals of oxidized fluorescence chemicals, implicating that during Cr(VI) treatment, a substantial amount of intracellular O_2 was consumed to generate $O_2^{-\cdot}$ and H_2O_2, and to produce local hypoxia [28]. These phenomena were confirmed by Gao et al., showing that levels of hypoxia-inducible factor 1 alpha (HIF-1α) increased in Cr(VI)-treated cells [29].

By demonstrating that DDH (also known as aldo-keto reductases) was sensitive to Cr(VI), our data suggested that DDH was involved in a Cr(VI)-mediated reduction/oxidation cascade. However, since the half-life of DDH had been estimated to be around 96–120 h [32], the abrupt degradation could be caused by the other mechanism. Using molecular replacement and X-ray diffraction as well as Rose Bengal-sensitized photo-oxidation methods, the active-site of DDH was found to contain histidine and lysine [33,34], suggesting a possibility that Cr(VI) could trigger protein oxidation and proteolysis of DDH [35]. Interestingly, DDH was also identified on the ER and Golgi [18,36], implying that DDH could be an intracellular oxidation sensor, and that Cr(VI)-associated oxidation could occur on the membrane structures (Supporting information Figure S2). It is thus worth noting that eEF2 and SAE2 are also located on the membrane structures (Supporting information Figure S3). Unlike DDH though, protein levels of eEF2, SAE2 as well as those of DRP1, c-Src, and c-Met increased following Cr(VI) treatment. Our previous study had shown that hypoxia increased levels of DRP1 and the phosphorylated DRP1. Increase of DRP1 protein level was regulated by eEF2, which in turn was monitored by SAE2 [16]. Phosphorylation of DRP, on the other hand, was mediated by AMPK [15]. In the current study, that both Cr(VI) and H_2O_2 promptly reduced DDH, but increased SAE2 expression suggested that DDH could play a role in the activation of eEF2 sumoylation, and the induction of differential expression of MSC markers under Cr(VI)-induced oxidation.

The increment of mesenchymal marker proteins and that of SAE2 and eEF2 took place within 6 h after addition of Cr(VI), and the effect was further augmented 4–10 folds, 48 h post-Cr(VI) challenge. The results indicated that the first wave of protein concentration increase (the direct response) could be induced by elevated eEF2 to maintain the efficacy of translation machinery, and the second wave of protein level upsurge (the delayed response) was triggered by the activation of transcription through the increased HIF-1α [29]. Cr(III) alone, however, did not immediately increase protein levels of MSC markers, suggesting that Cr(VI)-induced EMT might be resulted from the reduction of Cr(VI), and the accompanied generation of ROS. Results of vitamin C studies confirmed these theories, and indicated that the influence of Cr(III)-associated DNA adducts might take effect in the later phase [5,24,25].

Concomitant increase as well as synchronized augmentation of SAE2 and eEF2 expression further showed that SAE2 was required for the sumoylation of eEF2, and eEF2 sumoylation was essential for maintaining enzyme activity and translation efficacy [16]. This effect was extended into the delayed response phase. Together with the activated transcription, protein levels of MSC markers would increase significantly. Interestingly, Cr(VI) increased expression of c-Met and HER-2, but had no evident effect on that of epidermal growth factor receptor (EGFR), supporting a previous report that EGFR and the downstream effectors were crucial for renal regeneration [37]. It is thus worth noting that sumoylation of GTPase Rac1 facilitated HGF-associated cell migration [38]. Sumoylation of peroxisome proliferator-activated receptor-gamma (PPARγ) coactivator-1alpha (PGC-1α), on the other hand, reduced enzyme function and cell growth by curbing expression of genes crucial for cell metabolism and mitochondrial biogenesis [39]. Intriguingly, DDH possesses prostaglandin synthase activity to produce prostaglandin F2 alpha (PGF2α), which activates PPARγ [32]. With severe depletion of DDH, cells could have been taking alternative pathways for keeping themselves away from danger and stay alive.

Taken together, our data corresponded well with those findings and indicated that HK-2 cells could take five presumptive steps (as shown in Figure 5) in response to Cr(VI): (1) after entering the cells, Cr(VI) is reduced to Cr(III) via enzymes, e.g., TrxR and DDH, on intracellular membranes to generate ROS and H_2O_2 as well as a local hypoxia with substantial consumption of O_2; (2) Hypoxia increases SAE2 expression that mediates sumoylation of eEF2, and possibly Rac1 and PGC-1α; (3) Elevated eEF2 concentrations increases translation activity of MSC markers, which induce morphological changes of HK-2 cells; (4) In addition to protect nucleoli and rRNA synthesis, nuclear effect

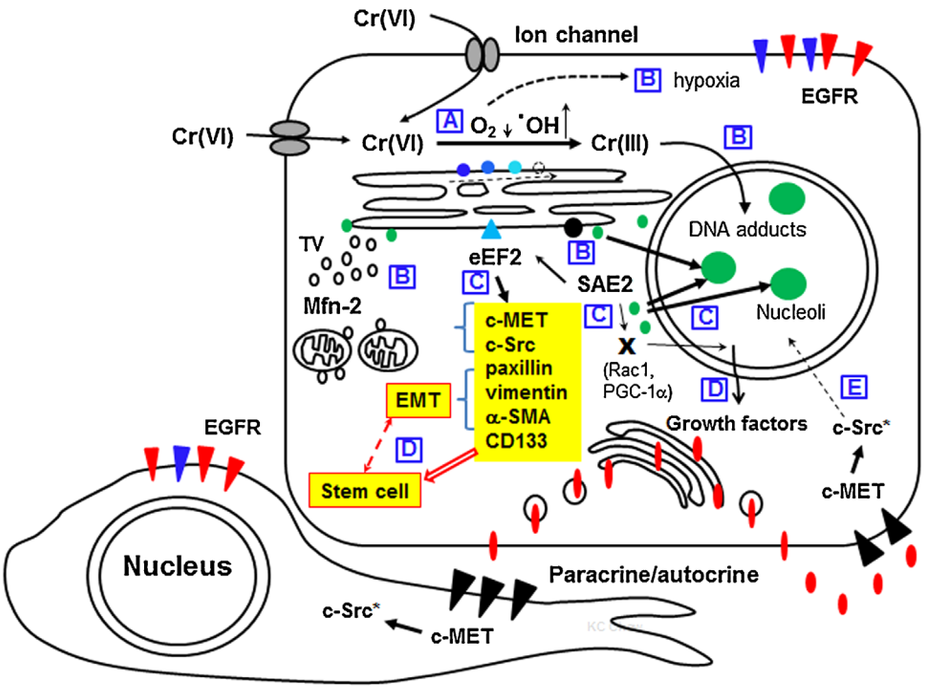

Figure 5. A simplified sketch of the five presumptive steps of HK-2 Cells in response to Cr(VI) challenge. (A) After entering the HK cells, Cr(VI) is promptly reduced to Cr(III) via enzymes, e.g., TrxR and DDH, on intracellular membranes to generate ROS and H_2O_2 as well as a local hypoxia with substantial expense of O_2. (B) The local hypoxia increases SAE2 expression, which then activates sumoylation of eEF2, and possibly Rac1 and PGC-1α. (C) Increment of eEF2 levels escalates translation activity of mesenchymal and stem cell markers, which subsequently induce morphological changes of HK-2 cells. (D) Other than protection of nucleoli and rRNA synthesis, nuclear effect of nucleolar DRP-1 alone or in association with that of probably PGC-1α could fortuitously increase expression of cell migration-related growth factors and cytokines. (E) Binding of the cell migration-related growth factors or cytokines to the respective receptors could enforce the Cr(VI) effect on EMT and synergistically activate cell motility as well as proliferation. Green circles, DRP1; $^{\cdot}OH$, hydroxyl radical; blue circles with fading colors, DDH and the oxidation-induced degradation forms of DDH, blue triangles; HER-2, red triangles; EGFR, black triangles; c-Met, gray ovals, ion channels.

of nucleolar DRP-1 in association with that of PGC-1α could fortuitously increase expression of cell migration-related growth factors and cytokines; (5) Binding of cell migration-related growth factors or cytokines to the respective receptors synergistically activates cell motility.

It should be noted, nonetheless, that other interpretations are possible. For instance, microRNAs, which regulate expression of MSC markers as well as that of cell migration-related growth factors, cytokines and the respective receptors, could be inactivated during reduction of Cr(VI) to Cr(III) [40]. As mentioned above, Cr(VI) does not affect expression of EGFR, but increases that of c-Met and HER-2. These data considered together with our current results clearly indicate that biological repair of the kidney is feasible. Although renal progenitor cells have been identified [6], reprogramming of these cells to differentiate into glomerular or tubular lineage is yet to be clarified. Screening for potential agents that are able to protect (using expression of DDH as an enzyme marker) (Supporting information Figure S4), and to induce differentiation of renal progenitors (using HK-2 as a cell model, and expression of Cx-43 as an enzyme marker) is being evaluated in an ongoing in vitro and in vivo studies.

In conclusion, our findings that Cr(VI) challenge increases expression of EMT and stem-cell markers indicate reprogramming of renal epithelial cells into mesenchymal or stem cells may be a natural response to the harsh environment, and such results have potential significance in the biological and medical implications for renal tubular epithelial cell regeneration and renal function restoration. Our current data clearly suggest that biological repair of the kidney is achievable and that the renal progenitors may be de-differentiated forms of epithelial origin. However, because HK-2 cells are HPV E6/E7-immortalized human kidney epithelial cells derived from proximal tubules, precautions must be taken for examining the in vivo effect of Cr(VI), in particular in the lack of data of glomerular epithelial cells. To achieve the goals of actual application to kidney biological repair, the in vivo study is warranted.

ACKNOWLEDGMENTS

This study was supported by the National Science Council (NSC 102-2320-B-005-006), Taipei, Taiwan, ROC, and by the Comprehensive Academic Promotion Projects (NCHU 1025025, Ministry of Education, Taiwan, ROC) and the Ministry of Education, under the ATU plan, Taiwan, ROC.

REFERENCES

1. Kalliomäki PL,Rahkonen E, Vaaranen V, Kalliomäki K, Aittoniemi K. Lung-retained contaminants, urinary chromium and nickel among stainless steel welders. Int Arch Occup Environ Health 1981;49:67–75.
2. Rosansky SJ, Huntsberger TL, Jackson K, Eggers P. Comparative incidence rates of end-stage renal disease treatment by state. Am J Nephrol 1990;10:198–204.
3. Linos A, Petralias A, Christophi CA, et al. Oral ingestion of hexavalent chromium through drinking water and cancer mortality in an industrial area of Greece–an ecological study. Environ Health 2011;10:50.
4. Wedeen RP, Qian L. Chromium-induced kidney disease. Environ. Health Prospect 1991;92:71–74.
5. Holmes AL, Wise SS, Wise JP, Sr. Carcinogenicity of hexavalent chromium. Ind J Med Res 2008;128:353–372.
6. Angelotti ML, Ronconi E, Ballerini L, et al. Characterization of renal progenitors committed toward tubular lineage and their regenerative potential in renal tubular injury. Stem Cells 2012;30:1714–1725.
7. Mendez MG, Kojima S, Goldman RD. Vimentin induces changes in cell shape, motility, and adhesion during the epithelial to mesenchymal transition. FASEB J 2010;24:1838–1851.
8. Desai VD, Hsia HC, Schwarzbauer JE. Reversible modulation of myofibroblast differentiation in adipose-derived mesenchymal stem cells. PLoS ONE 2014;9:e86865.
9. Menko AS, Bleaken BM, Libowitz AA, Zhang L, Stepp MA, Walker JL. A central role for vimentin in regulating repair function during healing of the lens epithelium. Mol Biol Cell 2014;25:776–790.
10. Bussolati B, Bruno S, Grange C, Ferrando U, Camussi G. Identification of a tumor-initiating stem cell population in human renal carcinomas. FASEB J 2008;22:3696–3705.
11. Rappa G, Fodstad O, Lorico A. The stem cell-associated antigen CD133 (Prominin-1) is a molecular therapeutic target for metastatic melanoma. Stem Cells 2008;26:3008–3017.
12. Chiang SF, Huang CY, Lin TY, Chiou SH, Chow KC. An alternative import pathway of AIF to the mitochondria. Int J Mol Med 2012;29:365–372.
13. Fang HY, Chang CL, Hsu SH, et al. ATPase family AAA domain-containing 3A is a novel anti-apoptotic factor in lung adenocarcinoma cells. J Cell Sci 2010;123:1171–1180.
14. Hsu NY, Ho HC, Chow KC, et al. Overexpression of dihydrodiol dehydrogenase as a prognostic marker of non-small cell lung cancer. Cancer Res 2001;61:2727–2731.
15. Chiang YY, Chen SL, Hsiao YT, et al. Nuclear expression of dynamin-related protein 1 in lung adenocarcinomas. Mod Pathol 2009;22:1139–1150.
16. Chen CY, Fang HY, Chiou SH, et al. Sumoylation of eukaryotic elongation factor 2 is vital for protein stability and anti-apoptotic activity in lung adenocarcinoma cells. Cancer Sci 2011;102:1582–1589.
17. Chen JT, Lin TS, Chow KC, et al. Cigarette smoking induces overexpression of HGF in type II pneumocytes and lung cancer cells Am J Respir Cell Mol Biol 2006;34:264–273..
18. Chiang YY, Wang SL, Yang CL, et al. Extracts of Koelreuteria henryi Dummer induce apoptosis and autophagy by inhibiting dihydrodiol dehydrogenase, thus enhancing anticancer effects. Int J Mol Med 2013;32:577–584.
19. You WC, Chiou SH, Huang CY, et al. Mitochondrial protein ATPase family, AAA domain containing 3A correlates with radioresistance in glioblastoma. Neuro-Oncology 2013;15:1342–1352.
20. Ishiyama M. A combined assay of cell viability and in vitro cytotoxicity with a highly water-soluble tetrazolium salt, neutral red and crystal violet. Biol Pharm Bull 1996;19:1518–1520.
21. Paglin S, Hollister T, Delohery T, et al. A novel response of cancer cells to radiation involves autophagy and formation of acidic vesicles. Cancer Res 2001;61:439–444.
22. Dasari V, Gallup M, Lemjabbar H, Maltseva I, McNamara N. Induction of Epithelial-mesenchymal transition in lung cancer: is tobacco the "smoking gun." Am J Respir Cell Mol Biol 2006;35:3–9.
23. Chen Z, Evans WH, Pflugfelder SC Li DQ. Gap junction protein connexin-43 serves as a negative marker for a stem cell-containing population of human limbal epithelial cells. Stem Cells 2006;24:1265–1273.
24. Dayan AD, Paine AJ. Mechanisms of chromium toxicity, carcinogenicity and allergenicity: Review of the literature from 1985 to 2000. Hum Exp Toxicol 1985;20:439–451.
25. Wise SS, Holmes AL, Wise JP, Sr. Hexavalent chromium-induced DNA damage and repair mechanisms. Rev Environ Health 2008;23:39–57.
26. Mackie KP, Nairn AC, Hampel G, Lam G, Jaffe EA. Thrombin and histamine stimulate the phosphorylation of elongation factor 2 in human umbilical vein endothelial cells. J Biol Chem 1989;264:1748–1753.
27. Myers JM, Antholine WE, Myers CR. The intracellular redox stress caused by hexavalent chromium is selective for proteins that have key roles in cell survival and thio redox control. Toxicology 2011;281:37–47.
28. Wang S, Leonard SS, Ye J, Ding M, Shi X. The role of hydroxyl radical as a messenger in Cr(VI)-induced p53 activation. Am J Physiol Cell Physiol 2000;279:C868–C875.
29. Gao N, Jiang BH, Leonard SS, et al. P38 Signaling-mediated hypoxia-inducible factor 1alpha and vascular endothelial growth factor induction by Cr(VI) in DU145 human prostate carcinoma cells. J Biol Chem 2002;277:45041–45048.
30. Kourí JB, Rojas L, Pérez E, Abbud-Lozoya KA. Modifications of Golgi complex in chondrocytes from osteoarthrotic (OA) rat cartilage. J Histochem Cytochem 2002;50:1333–1340.
31. Zwerger M, Kolb T, Richter K, Karakesisoglou I, Herrmann H. Induction of a massive endoplasmic reticulum and perinuclear space expansion by expression of lamin B receptor mutants and the related sterol reductases TM7SF2 and DHCR7. Mol Biol Cell 2010;21:354–368.
32. Huang KH, Lin TY, Chow KC, Chang HW, Chiang IP, Lee MC. Overexpression of aldo-keto reductase 1C2 is associated with disease progression in patients with prostate cancer. Histopathology 2010;57:384–394.
33. Shinoda M, Hara A, Nakayama T, Deyashiki Y, Sawada H. Modification of pig liver dimeric dihydrodiol dehydrogenase with diethylpyrocarbonate and by Rose Bengal-sensitized photooxidation: evidence for an active-site histidine residue. J Biochem 1992;112:834–839.
34. Hoog SS, Pawlowski JE, Alzari PM, Penning TM, Lewis M. Three-dimensional structure of rat liver 3 alpha-hydroxysteroid/dihydrodiol dehydrogenase: a member of the aldo-keto reductase superfamily. Proc Natl Acad Sci USA 1994;91:2517–2521.
35. Uchida K. Histidine and lysine as targets of oxidative modification. Amino Acids 2003;25:249–257.
36. Halim M, Yee DJ, Sames D. Imaging induction of cytoprotective enzymes in intact human cells: Coumberone, a metabolic reporter for human AKR1C enzymes reveals activation by panaxytriol, an active component of red ginseng. J Am Chem Soc 2008;130:14123–14128.
37. Regner KR, Nozu K, Lanier SM, et al. Loss of activator of G-protein signaling 3 impairs renal tubular regeneration

following acute kidney injury in rodents. FASEB J 2011;25:1844–1855.
38. Castillo-Lluva S, Tatham MH, Jones RC, et al. SUMOylation of the GTPase Rac1 is required for optimal cell migration. Nat Cell Biol 2010;12:1078–1085.
39. Rytinki MM, Palvimo JJ. SUMOylation attenuates the function of PGC-1alpha. J Biol Chem 2009;284:26184–26193.
40. Yang X, Zhang XF, Lu X, et al. MicroRNA-26a suppresses angiogenesis in human hepatocellular carcinoma by targeting hepatocyte growth factor c-Met pathway. Hepatology 2014;59:1874–1885.

SUPPORTING INFORMATION

Additional supporting information may be found in the online version of this article at the publisher's web-site.